Theoretical and Applied Mechanics

University of Illinois at Urbana-Champaign

TAM

TAM Report No. 1054
UILU-ENG-2004-6015
ISSN 0073-5264

Multi-scale modeling of solid rocket motors: Time integration methods from computational aerodynamics applied to stable quasi-steady motor burning

by

D. Scott Stewart
Kung-Chyun Tang
Sunhee Yoo
M. Quinn Brewster
Igor R. Kuznetsov

October 2004

Multi-Scale Modeling of Solid Rocket Motors: Time Integration Methods from Computational Aerodynamics Applied to Stable Quasi-Steady Motor Burning

D. Scott Stewart*, K.C. Tang†, Sunhee Yoo*, Quinn Brewster‡

and Igor R. Kuznetsov†

University of Illinois, Urbana, IL, 61801, USA

Here we consider the problem of efficiently computing the stable burn-back of a solid rocket motor when the motor is in the quasi-steady burning regime of operation. When the motor is modeled as a cavity that is filled with a compressible fluid with normal mass, momentum and energy injection from the solid propellant surface, the problem posed is a standard one in steady computational aerodynamics. For large rockets such as the space shuttle solid rocket booster, the problem of quasi-steady solid rocket motor ballistic flow is analogous to the steady aerodynamic flow past a large aircraft such as a Boeing 575 or F15 flying at speeds such that compressible flow must be fully accounted for. One can adopt advanced time integration strategies developed for application to commercial or military aircraft to the solid rocket motor grain burning to compute a series of realizations of steady flows as the grain burns back to near completion. The slow regression of the burning solid propellant surface is analogous to the motion of control surfaces on the aircraft as it moves through a controlled maneuver. Through the use of straightforward two-timing multi-scale asymptotic analysis we develop the reduced quasi-steady description of the quasi-steady burning regime for a model problem that is extensible to a full three-dimensional rocket. We discuss the application of now standard time integration methods from steady computational aerodynamics to the time-resolved computation of stable quasi-steady motor burning.

Nomenclature

ρ	gas density
u	gas velocity
c	sound speed
p	gas pressure
γ	ratio of specific heats
A	cross-section area
ρ_p	solid propellant density
S	cross-section perimeter
$\dot{r}$	regression rate of solid propellant
u_f	injection velocity of the combustion products
h_f	enthalpy of the combustion products

*Theoretical and Applied Mechanics.
†Center for Simulation of Advanced Rockets.
‡Mechanical and Industrial Engineering.

I. Introduction

The industry standard model for solid rocket motor combustion uses the compressible Euler equations for the gases with mass, momentum and energy injected normal to the solid propellant grain surface into the ballistic cavity. A representative derivation of this model used by industry has been given by Salita.[1,2] Successful motor operation has a long-lived stable burning regime. After the ignition phase the motor comes up to a nominally constant operating pressure and vents the combustion products through the nozzle until the final burn out phase. The stable burn is the longest operational phase of the motor where most of the acceleration from the motor thrust is achieved. For the space shuttle booster the time from ignition to burn out is on the order of about 100 seconds. During this phase the propellant surface regresses at approximately $10^{-2}\, m/sec$, while the maximum particle speed (and sound speed) in the ballistic core through the nozzle is on the order of $10^{3}\, m/sec$. The ratio of these two characteristic velocities, the regression velocity over the characteristic acoustic signalling velocity is a small parameter about $O(10^{-5})$. Thus on the time scale that would resolve acoustic events in the motor, the geometry of the ballistic cavity is frozen. Clearly if the motor is operating in the stable quasi-steady mode, one can compute a sequence of essentially steady flows with side wall injection in the ballistic core to simulate the stable quasi-steady burnout event.

The Center for Simulation of Advanced Rockets (CSAR) at the University of Illinois is a Department of Energy (DOE) program, funded by the Accelerated Strategic Computing Initiative, whose focus is to develop simulation capability for large solid rocket motors on modern large scale parallel computing platforms. At the heart of the project is the central task to simulate a full burn of a large motor. To accomplish this task (and indeed the same task for any large motor or spatially well-resolved small motor) it is essential to take full advantage of the properties of the stable quasi-steady burning phase to affect a realizable and efficient computation.

In the case of the steady aerodynamic flow past a large commercial aircraft such as a Boeing 575 or a military aircraft such as an F15, flight speeds are such that compressible flow must be fully accounted for. Designers that simulate aircraft face exactly the same challenge, and have almost an identical mathematical problem to solve. For aircraft in steady flight at speeds that require compressible flow modeling, the ratio of the speed of the change of control surfaces to the flow and sound speed over the aircraft is comparable to that cited above i.e. $O(10^{-5})$. One can wholly adopt the highly advanced time integration strategies developed for application to commercial or military aircraft to the solid rocket motor grain burning to compute a series of realizations of steady flow as the grain burns back to near completion. The slow regression of the burning solid propellant surface is analogous to the motion of control surfaces on the aircraft as it moves through a controlled manoeuver.

Through the use of straightforward two-timing, multi-scale asymptotic analysis we develop the reduced quasi-steady description of the quasi-steady burning regime for a model problem that is extensible to a full 3-D rocket. We show that if the quasi-steady burn is stable then it can be solved by time integrating a set of steady ballistic flows that are parametrically dependent on time, combined with the surface regression that evolves on the slow regression time scale. Thus we point out that the standard methods and strategies for computing steady computational aerodynamics, such as those developed by Jameson and colleagues,[4] can be directly applied to the computation of stable quasi-steady motor burning on the slow regression time scale.

Even at modest spatial resolutions a full motor simulation that marches at time increments defined by the CFL condition, is not practical, or at the current time realizable. It is a simple matter to convince oneself of this fact by the following estimates. Consider a rocket core with length L, average cross-sectional area A, final simulation time t_f, average spatial resolution $\triangle x$, number of spatial nodes in the main stream direction $N_x = L/\triangle x$, total of time steps for the simulation $N_t = t_f/\triangle t$. The relation between the time step and spatial increment defined by the CFL condition is given by $\triangle t = \alpha \triangle x/|u+c|$, where $|u+c|$ is the characteristic signalling velocity. The total operational count required to simulate the total burnout can be written as $N_{ops} = \beta N_t \times N_x^d$ where β is a geometry, machine and algorithm dependent constant and d is the dimension of the model ($d = 1, 2$, or 3). Combining these formulas obtains the formula $N_{ops} = (\beta/\alpha)[t_f|u+c|L^d]/[(\triangle x)^{d+1}]$. As an example for the space shuttle solid rocket booster, for a 30 meter rocket with 3 cm resolution in the stream direction (with $N_x = 1000$), with $|u+c| \sim 1000\ m/sec$, with $t_f = 100\, sec$, for a three-dimensional simulation with $d+1 = 4$, leads to the estimate $N_{ops} \sim (\beta/3\alpha) \times 10^{16}$. Even with advanced algorithms that could lead to small values of β, simple CFL-based time marching simulation is likely to be uncomputable, and the design parameter space unsearchable.

Thus we draw the simple conclusion that for the regimes of stable operation of a motor at pressures on the order of hundreds of atmospheres, marching at the CFL-prescribed time step is not viable for practical

computation; another strategy is required. Implementing a different time marching strategy on regression time scale can provide a reduction of total number of time steps significantly. The computational strategy is that associated with progressing through a series of quasi-steady states as defined by the intrinsic multi-scale asymptotic formulation for quasi-steady burning.

In what follows we briefly describe our simplified one-dimensional model, that can be used to study longitudinal dynamics of the rockets, but has all the elements in common with the three-dimensional Euler model to illustrate the main points. Then we derive reduced equations for quasi-steady burning for the model based on rational asymptotics. (The formulation of the reduced equation are essentially the same for a three-dimensional rocket.) We review some of the time marching strategies that are likely to be the most efficient for large scale rockets that employ parallel architecture drawn from established methods of computational aerodynamics suggested by Jameson[5] that can be directly implemented to compute the long-lived quasi-steady burn.

II. Multi-Scale Modeling of Solid Rocket Motors

A. A simplified Model of an SRM

The following model follows that posed by Salita,[1] and is slightly modified by us. Let the crossection of the ballistic section (gas core) of the rocket be given by $A(x,t)$, where x is the distance along the axis of the rocket and t is time. Then the governing equation for a rocket with a slowly varying cross section are

$$\frac{\partial \boldsymbol{u}}{\partial t} + \frac{\partial \boldsymbol{f}(\boldsymbol{u})}{\partial x} = \boldsymbol{s}(\boldsymbol{u})\,, \tag{1}$$

with

$$\boldsymbol{u} = \begin{bmatrix} \rho A \\ \rho u A \\ \rho e_T A \end{bmatrix}, \quad \boldsymbol{f}(\boldsymbol{u}) = \begin{bmatrix} \rho u A \\ (\rho u^2 + p)A \\ u(\rho e_T + p)A \end{bmatrix}, \quad \boldsymbol{s}(\boldsymbol{u}) = \begin{bmatrix} \rho_p \dot{r} S \\ p\frac{\partial A}{\partial x} \\ \rho_p \dot{r} S (h_f + \frac{1}{2}u_f^2) \end{bmatrix}, \tag{2}$$

where $e_T = p/(\rho(\gamma-1)) + u^2/2$ is the total energy, $S = 2\pi r$ is the perimeter, r is the effective cross-section radius, with $A = \pi r^2$. The propellant density is ρ_p, the enthalpy of the combustion products injected from the propellant surface is h_f and the injection velocity of the combustion products is $u_f = (\rho_p/\rho)\dot{r}$. Note that $r(x,t)$ is a variable that is determined through the addition of the surface regression evolution law

$$\frac{\partial r(x,t)}{\partial t} = k\, f(p,\rho,u) \tag{3}$$

that is prescribed specifying the combustion processes at the grain surface. The above equations hold in the region of the grain.

The model configuration is completed by the addition of nozzle that has area change. In such a region there is no side wall injection and the source terms for $\boldsymbol{s}$ are simply (by setting $\dot{r} = 0$)

$$\boldsymbol{s}(\boldsymbol{u}) = \begin{bmatrix} 0 \\ p\frac{\partial A}{\partial x} \\ 0 \end{bmatrix}. \tag{4}$$

B. Scaling

Here we consider scaling, such that the problem is posed on the scale of the longitudinal acoustics of the motor. Let a "c" subscript be a dimensional, characteristic scale. Choose the length scale to be L (the nominal length of the motor), let p_c be characteristic chamber pressure of steady state operation of the motor (i.e. on the order of 100 atmospheres), let ρ_c be a characteristic chamber density, choose the characteristic velocity be defined by the relation $V_c^2 = p_c/\rho_c$ so that the functional form of the governing equations is unchanged under scaling, and let the time scale be given by $t_c = L/V_c$.

Under the change of variables to dimensionless form the scaled version of the equations is the same as above except that $\boldsymbol{s}(\boldsymbol{u})$ is replaced by

$$\boldsymbol{s}(\boldsymbol{u}) = \begin{bmatrix} \epsilon f S \\ p\frac{\partial A}{\partial x} \\ \epsilon f S[Q + \frac{1}{2}\epsilon^2 f^2/\rho^2] \end{bmatrix}, \tag{5}$$

and the regression rate law becomes simply

$$\frac{\partial r}{\partial t} = \delta f\,, \tag{6}$$

where we identify the dimensionless parameter ϵ and δ as the dimensional ratios

$$\epsilon = \frac{\rho_p}{\rho_c} \times \frac{k}{V_c}\,, \quad \delta = \frac{k}{V_c}\,. \tag{7}$$

Note also that based on characteristics of typical solid propellant rocket motors, $\rho_p/\rho_c \sim 1750/5 \sim O(100)$, V_c is about the sound speed which is about $1000\,m/sec$ while the regression velocity is about $10^{-2}\,m/sec$ so that $k/V_c \sim O(10^{-5})$, with $\epsilon \sim 10^{-3}$ and $\delta \sim 10^{-5}$. Also we should note that $Q = h_f/V_c^2$ is $O(1)$.

Measured on the acoustic time scale, the burning surface evolves with $O(1)$ changes to its configuration on an $O(1/\delta) \sim 10^5$ time scale, a very long time indeed. The time required to observe changes in the shape of the grain is so long that resolved time evolution on the acoustic time scale is essentially, in practical terms, uncomputable for a large rocket. The only way to compute the configuration changes in a straightforward way is to compute a series of essentially (quasi-) steady states, and then make configuration changes on the time scale on the order of the regression rate.

What follows next is a simple but rigorous derivation of the reduced equations for quasi-steady burning in SRMs, explained in the context of this simplified model.

III. The Quasi-Steady Burn Approximation

Here we consider the following limit. Let ϵ be $O(1)$ on the scale of δ and simply consider the limit as $\delta \to 0$. Further let $t = t_0$ (we will drop the zero subscript subsequently) be the "fast" acoustic time scale, and let $\tau = \delta t$ be the "slow" regression (shape change) time scale. For a multiple-time scale expansion of the form

$$\boldsymbol{u} = \boldsymbol{u}^{(0)}(x,t,\tau) + \delta \boldsymbol{u}^{(1)}(x,t,\tau) + \dots\,. \tag{8}$$

one calculates

$$\frac{\partial \boldsymbol{u}}{\partial t} = \frac{\partial \boldsymbol{u}^{(0)}}{\partial t} + \delta \frac{\partial \boldsymbol{u}^{(0)}}{\partial \tau} + \delta \frac{\partial \boldsymbol{u}^{(1)}}{\partial t} + \dots\,, \tag{9}$$

$$\frac{\partial \boldsymbol{f}}{\partial x} = \frac{\partial \boldsymbol{f}(\boldsymbol{u}^{(0)}(x,t,\tau) + \delta \boldsymbol{u}^{(1)}(x,t,\tau) + \dots)}{\partial x} = \frac{\partial \boldsymbol{f}(\boldsymbol{u}^{(0)})}{\partial x} + \delta \frac{\partial}{\partial x}\left[\frac{\partial \boldsymbol{f}(\boldsymbol{u}^{(0)})}{\partial \boldsymbol{u}} \boldsymbol{u}^{(1)}\right] + \dots\,, \tag{10}$$

and

$$\boldsymbol{s}(\boldsymbol{u}) = \boldsymbol{s}(\boldsymbol{u}^{(0)}) + \dots\,. \tag{11}$$

The regression rate law expansion

$$\frac{\partial r}{\partial t}|_t = \frac{\partial r^{(0)}}{\partial t} + \delta\left[\frac{\partial r^{(1)}}{\partial t} + \frac{\partial r^{(0)}}{\partial \tau}\right] + \dots = \delta\left[f(p^{(0)}, \rho^{(0)}, u^{(0)}) + \dots\right]. \tag{12}$$

The leading order, $O(1)$ formulation in the propellant grain domain is then expressed as

$$\frac{\partial \boldsymbol{u}^{(0)}}{\partial t} + \frac{\partial \boldsymbol{f}(\boldsymbol{u}^{(0)})}{\partial x} = \boldsymbol{s}(\boldsymbol{u}^{(0)})\,, \tag{13}$$

$$\boldsymbol{s}(\boldsymbol{u}^{(0)}) = \begin{bmatrix} \epsilon f^{(0)} S^{(0)} \\ p^{(0)} \frac{\partial A^{(0)}}{\partial x} \\ \epsilon f^{(0)} S^{(0)} [Q + \frac{1}{2}\epsilon^2 \frac{(f^{(0)})^2}{(\rho^{(0)})^2}] \end{bmatrix}, \tag{14}$$

with the leading order regression, effectively motionless, as

$$\frac{\partial r^{(0)}}{\partial t} = 0\,. \tag{15}$$

In the nozzle region, Eq. (13) holds with $\boldsymbol{s}(\boldsymbol{u})$ identified by Eq. (4).

This leading order system has fast time dynamics, with injection from the side-wall for a fixed grain geometry. Quasi-steady motor burning is the special case when the leading order solution is steady on the fast, acoustic time scale. We turn to that case next.

A. Definition of Quasi-Steady Burning

The special solution of this system is the steady burning solution that has $t_0 = t$, and sets $\partial/\partial t_0 = 0$, in which case one must solve the following ordinary differential equations

$$\frac{\partial \boldsymbol{f}(\boldsymbol{u}^{(0)})}{\partial x} = \boldsymbol{s}(\boldsymbol{u}^{(0)})\ . \tag{16}$$

To these equations we add the boundary condition at the head end $u = 0$ at $x = 0$. Specification of the head end pressure and density would provide enough information to allow us to integrate Eq. (16) forward to determine profiles in the grain region. These values are determined by insisting that at the entrance to the inert nozzle the state variables, i.e. ρ, u and p and hence the mass flux are continuous, and that the nozzle is an isentropic expansion with a sonic point at the throat. Next we give the detailed description of such calculation.

B. Calculation of Steady Flow Through Rocket with Slowly Varying Cross-Section

Here we consider the calculation of the steady flow in a rocket with a slowly varying grain and nozzle shape. Calculation of the steady flow with steady side wall injection that is a function of the state, reduces to the solution of a nonlinear eigenvalue problem.

The steady equations that govern both the grain and nozzle section can be represented by (dropping the zero superscript if we represent the quasi-steady state) as

$$\frac{d\boldsymbol{f}(\boldsymbol{u})}{dx} = \boldsymbol{s}(\boldsymbol{u})\,, \quad \boldsymbol{f}(\boldsymbol{u}) = \begin{bmatrix} \rho u A \\ (\rho u^2 + p)A \\ u(\rho e_T + p)A \end{bmatrix} \equiv \begin{bmatrix} f_1 \\ f_2 \\ f_3 \end{bmatrix}, \tag{17}$$

where $\boldsymbol{s}(\boldsymbol{u})$ is given by Eq. (2c) or Eq. (4) in the grain or nozzle segment respectively.

To integrate these equations from the head end of the rocket $x = 0$, we need to prescribe the values of f_i at $x = 0$. We know that particle velocity u is zero at the head end, which sets $f_1(0) = f_3(0) = 0$, and $f_2(0) = p(0)A(0)$. The value of area function $A(x)$ is assumed to be known. To start the integration, we make a guess for the pressure at the head end $p(0)$ and integrate to the inlet of the nozzle $x = x_{inlet}$. The primitive states can be calculated from the algebraic formulas

$$\begin{aligned} p &= \frac{f_2 + \sqrt{f_2^2\gamma^2 + 2f_1 f_3(1-\gamma^2)}}{A(1+\gamma)}\,, \\ u &= f_2/f_1 - A/f_1 p\,, \rho = f_1/(Au)\,. \end{aligned} \tag{18}$$

The Mach number at the inlet is given by

$$M_{inlet} = \sqrt{\gamma \frac{p_{inlet}}{\rho_{inlet}}}\,.$$

For the same point, we calculate the inlet Mach number from the area-Mach number relation[6] for the nozzle, here designated by a plain M as

$$\frac{A_{inlet}}{A_{throat}} = \left(\frac{2}{\gamma+1}\right)^{\frac{\gamma+1}{2(\gamma-1)}} \frac{1}{M}\left(1+\frac{\gamma-1}{2}M^2\right)^{\frac{\gamma+1}{2(\gamma-1)}}, \tag{19}$$

where the nozzle contraction ratio A_{throat}/A_{inlet} is prescribed. Iterations on $p(0)$ are repeated until $RES \equiv (M_{inlet} - M) < ERRABS$ or until the difference between two successive guesses for the head pressure is less than ERRREL.

Once iterations converge, the correct solution is found in the domain from the head end to the nozzle inlet. In order to obtain solution in the nozzle part of the domain, we employ algebraic nozzle relations[6] as follows. Using inlet values as a starting point, at the neighboring grid point inside the nozzle, area ratio is calculated. Based on that ratio, and inlet values, the values of primitive variables at the location of the current grid point are obtained.

Figure 1 shows an example of solid rocket motor geometry with a steady state primitive variable profiles computed by ODE solver "STEADY" and those computed from the direct numerical solution of a relaxation to quasi-steady state of the fully unsteady model. The two solutions fall on top of each other. Both simulations were performed on a grid of 800 nodes.

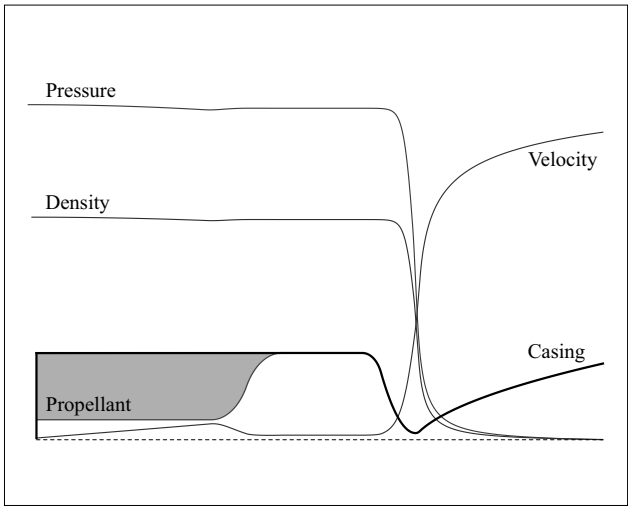

Figure 1. Comparison of primitive variable profiles in the rocket booster obtained by direct numerical solution of unsteady governing equations (relaxed to a steady state) and by ODE solver STEADY.

Main iterations for steady state solver STEADY were performed with IMSL routine DZREAL, EPS $= 1 \times 10^{-15}$, ERRABS $= 1 \times 10^{-15}$, ERRREL $= 1 \times 10^{-15}$, ETA $= 1 \times 10^{-12}$. The root of Eq. (19) is found with DZBREN ERRABS $= 1 \times 10^{-15}$, ERRREL $= 1 \times 10^{-15}$. Subroutine DIVPRK was implemented to solve Eq. (17) from the head end to the nozzle inlet, with tolerance parameter set to TOLR $= 5 \times 10^{-3}$. Second order accuracy of the solver is verified by substituting the solution back into the governing equations and evaluating the residuals.

The direct numerical solution of our model was accomplished by using a hybrid level set algorithm[8] Wave Tracker (WT) to evolve the grain geometry and a high resolution WENO scheme[9] that uses the method of lines and 3rd order Runga-Kutta scheme. The versions of these algorithms were recently implemented for application to multi-material hydrodynamics and shock physics simulations.[10] CFL number was set to 0.9 and initial condition was an output from ODE solver STEADY perturbed by 5%.

A combined WT/STEADY solver was used to perform complete motor burnout tests to estimate an upper bound speedup of the total simulation. For each grain configuration, STEADY is used to compute steady state solution. Pressure distribution is then used to evaluate the burn rate using

$$\dot{r} = a(\hat{p})^b, \tag{20}$$

where $\hat{p}$ is local pressure measured in atmospheres, $a = 2.44 \times 10^{-3}$ and $b = 0.35$. Based on calculated burn rate, WT is used to progress the propellant surface into a new configuration at the next time step.

Table 1 presents burnout test results. Here N_{pts} is a number of grid points, N_{iter} is a number of time steps (geometry updates) taken by Wave Tracker in order to reach final burn out time of 140 seconds, $\triangle t$ is the time step imposed by Wave Tracker CFL condition, and T_{sim} is total simulation run time (in seconds) on a single AMD 2000+ 1.67GHz processor.

For $N_{pts} = 200$ points, the Wave Tracker time step ($\triangle t = 0.0275\, sec$) requires approximately 5×10^3 iterations (time steps) for a complete burnout, whereas Euler solver time step at the same spatial resolution would be $\triangle t_e = 7 \times 10^{-6}\, sec$, requiring 2×10^7 iterations. This gives an estimate of the upper bound for a speedup of the burnout simulation performed as a series of quasi-steady state calculations compared to

the direct Euler solver stepping with gas dynamics-prescribed CFL condition. Such estimate, expressed as a ratio of number of time steps required, in this particular case is approximately 4×10^3 times.

Table 1. Burn-out test results

N_{pts}	N_{iter}	$\triangle t$	T_{sim}
200	5,095	0.0275	522
400	10,444	0.0138	2,432
800	20,241	0.00069	11,011

Test geometry of the booster is chosen to be 14 meters long and 3 meters wide. Reduction of the motor length allows us to reduce the cost of the simulation. Since the goal of this test is to estimate the speedup, not to build a precise model of SRM, such modification of geometry is admissible.

Another restriction that we apply to our test geometry is smoothness. The function $A(x)$, along with its derivative $A'(x)$ has to be continuous. One must recognize that area function is introduced to modify the governing equations in order to account for two-dimensional geometry of the rocket motor within a one-dimensional model. Such quasi-one dimensional mathematical model is accurate and satisfies all the modeling assumptions, but when discretized can produce numerically generated discontinuity to the source terms near points where $A(x)$ is not smooth. To achieve desired accuracy of direct solver, it is sufficient to require that $A(x)$ is C^1 continuous.

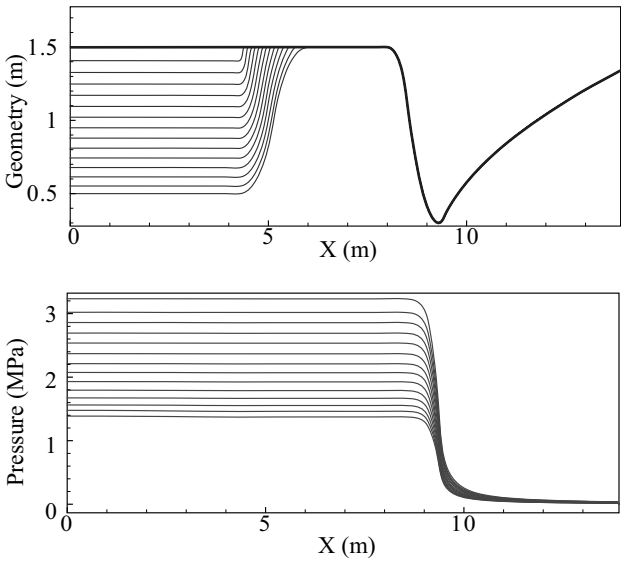

Figure 2. Burnout test of 140 sec.

Figure 2 presents time evolution of grain geometry and pressure. Frames are recorded at time intervals of 10 *sec* (14 frames for entire burnout test). As the propellant grain burns out, the internal radius of the cavity increases, leading to an increase in burning area. At the same time, the length of the propellant grain decreases, leading to a decrease of the burning area. The choice of the initial geometry of the grain defines the balance between the two processes. In our test case, gradual burning surface area increase leads to increase in chamber pressure.

C. Summary of the Reduced Equations Appropriate for Quasi-Steady Motor Burning

If we assume that the flow is steady on the fast-time scale but allow for changes on the slow time scale, then steady flow equations

$$\frac{\partial \boldsymbol{f}(\boldsymbol{u}^{(0)})}{\partial x} = \boldsymbol{s}(\boldsymbol{u}^{(0)}) \tag{21}$$

hold in the ballistic core. The regression rate law expansion at $O(\delta)$ given by Eq. (12) is expressed uniformly as

$$\frac{\partial r^{(0)}}{\partial t} = \delta f(\rho^{(0)}, p^{(0)}, u^{(0)})\,. \tag{22}$$

These reduced equations govern leading order quasi-steady rocket motor burn. The balance equations (21) depend parametrically on the slow time, δt. These equations are not the fully unsteady equations. A separate time integration strategy must be devised to achieve their solution. If the quasi-steady flow is unstable on

the fast, acoustic time scale, then the solutions achieved by the integration of this system are "not" the physically appropriate ones. But if the quasi-steady flow is stable on the acoustic time scale, then a time integration method can be used that is appropriate to compute steady compressible, transonic flows. Then methods developed largely for aircraft are the appropriate ones to consider. These will be discussed below.

We make a comment about stability of these quasi-steady flows. Since the quasi-steady burn evolves on the slow time scale, it is steady on the fast, acoustic time scale. On the fast time scale the geometry of the rocket, here $A(x,t)$ is frozen in time. So there is a possibility that the rocket can slowly burn into a geometry where the quasi-steady solution is no longer stable and a transition to instability occurs.

The detailed analysis of acoustic instabilities is not within the scope of our present discussion, and will be addressed in a sequel to this work.

IV. Summary of Basic Strategies from Computational Aerodynamics

Here we present a summary of some conclusions and strategies from computational aerodynamics that can be applied to integration of the quasi-steady equations for large scale motor. Recently at a United States Air Force Office of Scientific Research Workshop on "Advances and Challenge in Time-Integration of PDEs" held at Brown University in August, 2003, A. Jameson, Stanford University presented a summary of modern methods and strategies from computational aerodynamics developed specifically for large scale machines in compressible flow. Here we recount some of his conclusions[5] that we believe identify the best strategies that can be applied to large scale motor simulation. One is referred to recent monograph,[7] and Jameson's original article on multigrid.[4]

If one needs only to compute steady flows (in our case as levels in the temporal discretization of the dynamics on the slow regression time scale), a "fast" steady state solver is always needed, even for a fully implicit scheme. The simplest method is to compute solutions to the full unsteady Euler equation until a new steady state is achieved; but this is not efficient since there is a significant relaxation time required for pressure equilibration, often requiring at least 1000 pressure wave traverses through the structure. Alternatively one can identify a preconditioner that multiplies the steady state homogenous operator and add to the homogenous spatial operator a pseudo-time derivative of the dependent variables. Then the steady state is achieved by relaxation to the steady state in pseudo-time. One can consider fully implicit schemes. These schemes have the property that a fully nonlinear set of algebraic equations results, and even linear solve of these equations requires the inversion of a full matrix. The implicit schemes based on backwards time differencing that is linearized by an approximate factorization to give a alternating direction implicit scheme, do not easily lead to parallelization, as the entire grid must be updated sequentially on a sweep.

A preferred scheme that is easy to implement, has good accelerated convergence properties and can be easily made parallel is the multigrid method, with a modified Runge-Kutta time integration. The idea is to take large time steps on a sequence of coarse grids, and interpolate between the finer and coarser meshes with a sequence of time steps that do not violate the stability restriction. Next we show that a multigrid scheme can produce accelerated time integration.

A. Multigrid with RK Integration

In a quasi-one dimensional formulation, the fastest and the most accurate way to obtain a steady state solution is to solve steady state equations which, as we have shown, can be done by iterating on the head end pressure. In two and three dimensions, there is no such simple and straight-forward way to solve the system of steady governing equations, hence we need to use other methods, such as multigrid, to obtain steady state solution.

Here we test multigrid method[3,4] in one dimension in order to verify its applicability to the SRM problem, demonstrate the speedup of the simulation and estimate possible benefits of applying it to multi-dimensional problem.

Multigrid method effectively accelerates convergence to the steady state by solving unsteady governing equations on successively coarser meshes that allow larger time steps. We used the V-cycle with 4th order modified Runge-Kutta time integration[4,5] on each grid level.

For our test geometry, minimum number of grid points that allow us to capture all significant geometry details, such as nozzle throat width, was considered to be 200. If maximum desired resolution is around one centimeter, we can allow for three levels of refinement, with 4-grid level system of 200, 400, 800, 1600 grid

points.

As soon as the algorithm was implemented, we observed that numerical error generated at locations where function $A(x)$ was not C^2 smooth was magnified in the multigrid simulation which resulted in slow, or no convergence to the steady state solution. To remedy this difficulty, we reformulated the governing equations so that all area-related terms were only present as source terms, and did not appear in the flux calculation. In this way we excluded possible source of singularity due to geometry from the flux calculation.

$$\boldsymbol{u} = \begin{bmatrix} \rho \\ \rho u \\ \rho e_T \end{bmatrix}, \quad \boldsymbol{f}(\boldsymbol{u}) = \begin{bmatrix} \rho u \\ \rho u^2 + p \\ u(\rho e_T + p) \end{bmatrix}, \quad \boldsymbol{s}(\boldsymbol{u}) = \frac{1}{A} \begin{bmatrix} \rho_p \dot{r} S - \rho u \frac{dA}{dx} \\ -\rho u^2 \frac{dA}{dx} \\ \rho_p \dot{r} S (h_f + \frac{1}{2} u_f^2) - \frac{dA}{dx}(u(\rho e_T + p) \end{bmatrix}. \tag{23}$$

Secondly, we changed geometry such that resulting function A(x) is C^2 smooth by using hyperbolic functions to represent the shape of propellant grain and nozzle (Fig. 3). Grain part of the A(x) is defined by $tanh(x) = (e^{2x} - 1)/(e^{2x} + 1)$, and nozzle part is defined by $sech(x) = 2/(e^x + e^{-x})$.

We must emphasize that these remedies are only needed in one-dimensional formulation, where function $A(x)$ is present and source terms are modified to account for chamber area change. In higher dimensions, area change is introduced by boundary conditions of the problem and does not enter the governing equations. Therefore, in two- and three-dimensional, current multigrid model can be applied to arbitrary solid propellant grain and nozzle shapes, without smoothness restrictions.

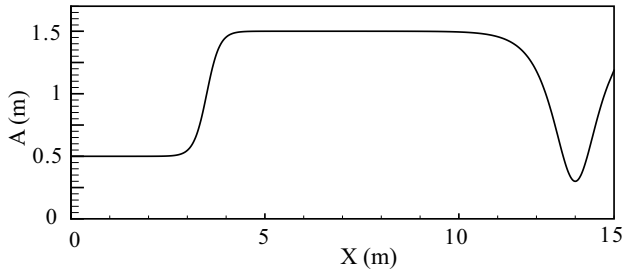

Figure 3. Area function $A(x)$ used for multigrid calculations.

"Ideal" multigrid algorithm figure of merit can be estimated as follows. Following Jameson,[5] for the V-cycle the computational cost of one multigrid time step (cycle) is evaluated to be

$$\begin{aligned} 1 + \frac{1}{2} + \frac{1}{4} + \ldots &< 2 \quad \text{in one dimension,} \\ 1 + \frac{1}{4} + \frac{1}{16} + \ldots &< \frac{4}{3} \quad \text{in two dimensions,} \\ 1 + \frac{1}{8} + \frac{1}{64} + \ldots &< \frac{8}{7} \quad \text{in three dimensions.} \end{aligned}$$

The effective time step of one multigrid cycle is

$$\triangle T = (1 + 2 + 4 + 8 + \ldots)\triangle t\,,$$

where $\triangle t$ is the time step determined by CFL condition for the finest grid. Therefore we can estimate the figure of merit, or speedup of calculating the steady state, for such ideal multigrid algorithm in case of linear convergence, in one dimension as

$$\sum^{n} 2^i / \sum^{n} 2^{-i}\,,$$

which in case of four grid levels ($n = 3$) gives speedup of 8 times.

In reality, due to additional costs associated with transferring information between grid levels and with possible non-linear convergence of the problem at hand, figure of merit is smaller. Nevertheless, the general fact remains that with higher number of grid levels performance of the multigrid method increases, and that figure of merit for three-dimensional calculation is higher that that for two-dimensional one, which is higher that that for one-dimensional problem.

Figure 4 represents a comparison of number of iterations required for attaining a steady-state solution of desired accuracy for one-grid and three-grid simulations. Starting from initial condition that is 1% off the exact solution, calculation on one grid with 800 nodes required approximately 4 times more iterations than calculation with three grid levels (200, 400, 800) to converge to a steady solution. The L_2 norm was calculated as

$$L_2 = \sqrt{\sum^{n} (\hat{p}_i - p_i)^2}\,,$$

where p_i is pressure at grid point i and $\hat{p}_i$ is the pressure at grid point i calculated by STEADY.

Time speedup of up to four grid levels is presented on Fig. 5. Convergence criterion was imposed as L_2 norm of the change between two successive multi-grid time steps being less than preset tolerance (10^{-8}). We see that actual time speedup of the simulation is 3 times, less that expected for the best-case scenario. Nevertheless it is a good acceleration result, which is predicted to become better as we go from one dimension to two and three dimensions, as well as if the number of grid levels is increased.

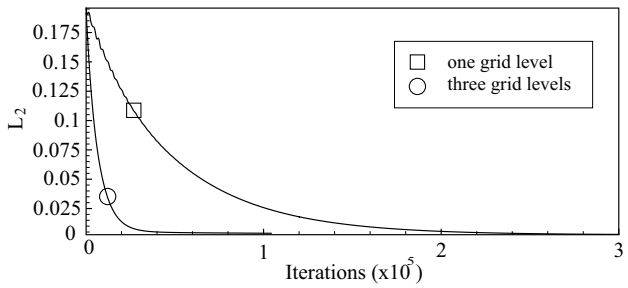

Figure 4. Error (L_2) as function of iteration number, for one grid of 800 nodes and three grid levels (200, 400, 800).

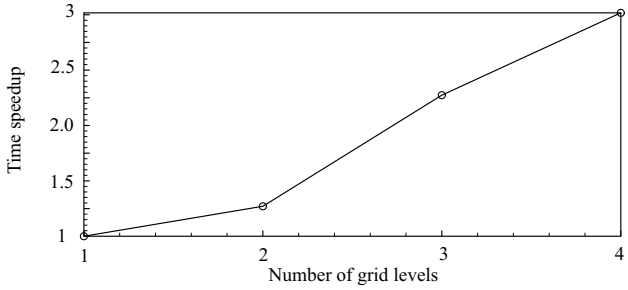

Figure 5. Time speedup of convergence to a steady state as function of number of grid levels.

Acknowledgments

The University of Illinois Center for Simulation of Advanced Rockets research program is supported by the US Department of Energy through the University of California under sub contract B341494. D. S. Stewart and S. Yoo have also been supported by the US Air Force Research Laboratory, Munitions Directorate under sub contract F08630-00-1-0002, and by US Air Force Scientific Research, Physical Mathematics under sub contract F49620-03-1-0048.

References

[1]Salita, M., "Verification of Spatial and Temporal Pressure Distribution in Segmented Solid Rocket Motors," AIAA paper 89-0298, *27th Aerospace Sciences Meeting*, Reno, Nevada, Jan. 9-12, 1989.

[2]Salita, M., "Closed-Form Analytical Solutions for Fluid Mechanical, Thermomechanical, and Thermal Processes in Solid Rocket Motors," AIAA paper 98-3965, *34th Joint Propulsion Conference and Exhibit*, Cleveland, Ohio, Jul. 13-15, 1998.

[3]Fedorenko, R.P., "A Relaxation Method for Solving Elliptic Difference Equations," *USSR Comput. Math. and Phys.*, 1:1092–1096, 1961.

[4]Jameson, A., "Solution of the Euler Equations by a Multigrid Method," *Applied Math. and Computation*, Vol. 13, 1983, pp. 327-356.

[5]Jameson, A., "Time-Integration Methods in Computational Aerodynamics," *AFOSR Work Shop on Advances and Challenges in Time-Integration of PDEs*, Providence, RI, Aug.18, 2003.

[6]Sutton, G.P. and Biblarz, O., *Rocket Propulsion Elements*, Interscience; 7 edition (December 15, 2000), p. 45.

[7]Erberle, A., "Numerical Solutions of the Euler Equations for Steady Flow Problems," *Notes on Numerical Fluid Mechanics*, Vol. 34, Vieweg (1992).

[8]Yoo, S. and Stewart, D.S., "A Hybrid Level-Set Method for Modeling Detonation and Combustion Problems in Complex Geometries," to appear in *Combust. Theory and Modelling.*

[9]Xu, S., Aslam, T. and Stewart, D. S., "High Resolution Numerical Simulation of Ideal and Non-Ideal Compressible Reacting Flows with Embedded Internal Boundaries," *Combust. Theory and Modelling*, Vol. 1, No. 1, 1997.

[10]Stewart, D.S., Yoo, S. and Wescott, B., "High Resolution Methods for Multi-Material Simulations", in preparation.

List of Recent TAM Reports

No.	Authors	Title	Date
968	Riahi, D. N.	Effects of rotation on convection in a porous layer during alloy solidification—Chapter 12 in *Transport Phenomena in Porous Media* (D. B. Ingham and I. Pop, eds.), 316–340 (2002)	Apr. 2001
969	Damljanovic, V., and R. L. Weaver	Elastic waves in cylindrical waveguides of arbitrary cross section—*Journal of Sound and Vibration* (submitted)	May 2001
970	Gioia, G., and A. M. Cuitiño	Two-phase densification of cohesive granular aggregates—*Physical Review Letters* **88**, 204302 (2002) (in extended form and with added co-authors S. Zheng and T. Uribe)	May 2001
971	Subramanian, S. J., and P. Sofronis	Calculation of a constitutive potential for isostatic powder compaction—*International Journal of Mechanical Sciences* (submitted)	June 2001
972	Sofronis, P., and I. M. Robertson	Atomistic scale experimental observations and micromechanical/ continuum models for the effect of hydrogen on the mechanical behavior of metals—*Philosophical Magazine* (submitted)	June 2001
973	Pushkin, D. O., and H. Aref	Self-similarity theory of stationary coagulation—*Physics of Fluids* **14**, 694–703 (2002)	July 2001
974	Lian, L., and N. R. Sottos	Stress effects in ferroelectric thin films—*Journal of the Mechanics and Physics of Solids* (submitted)	Aug. 2001
975	Fried, E., and R. E. Todres	Prediction of disclinations in nematic elastomers—*Proceedings of the National Academy of Sciences* **98**, 14773–14777 (2001)	Aug. 2001
976	Fried, E., and V. A. Korchagin	Striping of nematic elastomers—*International Journal of Solids and Structures* **39**, 3451–3467 (2002)	Aug. 2001
977	Riahi, D. N.	On nonlinear convection in mushy layers: Part I. Oscillatory modes of convection—*Journal of Fluid Mechanics* **467**, 331–359 (2002)	Sept. 2001
978	Sofronis, P., I. M. Robertson, Y. Liang, D. F. Teter, and N. Aravas	Recent advances in the study of hydrogen embrittlement at the University of Illinois—Invited paper, Hydrogen–Corrosion Deformation Interactions (Sept. 16–21, 2001, Jackson Lake Lodge, Wyo.)	Sept. 2001
979	Fried, E., M. E. Gurtin, and K. Hutter	A void-based description of compaction and segregation in flowing granular materials—*Continuum Mechanics and Thermodynamics*, in press (2003)	Sept. 2001
980	Adrian, R. J., S. Balachandar, and Z.-C. Liu	Spanwise growth of vortex structure in wall turbulence—*Korean Society of Mechanical Engineers International Journal* **15**, 1741–1749 (2001)	Sept. 2001
981	Adrian, R. J.	Information and the study of turbulence and complex flow—*Japanese Society of Mechanical Engineers Journal B*, in press (2002)	Oct. 2001
982	Adrian, R. J., and Z.-C. Liu	Observation of vortex packets in direct numerical simulation of fully turbulent channel flow—*Journal of Visualization*, in press (2002)	Oct. 2001
983	Fried, E., and R. E. Todres	Disclinated states in nematic elastomers—*Journal of the Mechanics and Physics of Solids* **50**, 2691–2716 (2002)	Oct. 2001
984	Stewart, D. S.	Towards the miniaturization of explosive technology—Proceedings of the 23rd International Conference on Shock Waves (2001)	Oct. 2001
985	Kasimov, A. R., and Stewart, D. S.	Spinning instability of gaseous detonations—*Journal of Fluid Mechanics* (submitted)	Oct. 2001
986	Brown, E. N., N. R. Sottos, and S. R. White	Fracture testing of a self-healing polymer composite—*Experimental Mechanics* (submitted)	Nov. 2001
987	Phillips, W. R. C.	Langmuir circulations—*Surface Waves* (J. C. R. Hunt and S. Sajjadi, eds.), in press (2002)	Nov. 2001
988	Gioia, G., and F. A. Bombardelli	Scaling and similarity in rough channel flows—*Physical Review Letters* **88**, 014501 (2002)	Nov. 2001
989	Riahi, D. N.	On stationary and oscillatory modes of flow instabilities in a rotating porous layer during alloy solidification—*Journal of Porous Media* **6**, 1–11 (2003)	Nov. 2001
990	Okhuysen, B. S., and D. N. Riahi	Effect of Coriolis force on instabilities of liquid and mushy regions during alloy solidification—*Physics of Fluids* (submitted)	Dec. 2001

List of Recent TAM Reports (cont'd)

No.	*Authors*	*Title*	*Date*
991	Christensen, K. T., and R. J. Adrian	Measurement of instantaneous Eulerian acceleration fields by particle-image accelerometry: Method and accuracy—*Experimental Fluids* (submitted)	Dec. 2001
992	Liu, M., and K. J. Hsia	Interfacial cracks between piezoelectric and elastic materials under in-plane electric loading—*Journal of the Mechanics and Physics of Solids* **51**, 921–944 (2003)	Dec. 2001
993	Panat, R. P., S. Zhang, and K. J. Hsia	Bond coat surface rumpling in thermal barrier coatings—*Acta Materialia* **51**, 239–249 (2003)	Jan. 2002
994	Aref, H.	A transformation of the point vortex equations—*Physics of Fluids* **14**, 2395–2401 (2002)	Jan. 2002
995	Saif, M. T. A, S. Zhang, A. Haque, and K. J. Hsia	Effect of native Al_2O_3 on the elastic response of nanoscale aluminum films—*Acta Materialia* **50**, 2779–2786 (2002)	Jan. 2002
996	Fried, E., and M. E. Gurtin	A nonequilibrium theory of epitaxial growth that accounts for surface stress and surface diffusion—*Journal of the Mechanics and Physics of Solids* **51**, 487–517 (2003)	Jan. 2002
997	Aref, H.	The development of chaotic advection—*Physics of Fluids* **14**, 1315–1325 (2002); see also *Virtual Journal of Nanoscale Science and Technology*, 11 March 2002	Jan. 2002
998	Christensen, K. T., and R. J. Adrian	The velocity and acceleration signatures of small-scale vortices in turbulent channel flow—*Journal of Turbulence*, in press (2002)	Jan. 2002
999	Riahi, D. N.	Flow instabilities in a horizontal dendrite layer rotating about an inclined axis—*Journal of Porous Media*, in press (2003)	Feb. 2002
1000	Kessler, M. R., and S. R. White	Cure kinetics of ring-opening metathesis polymerization of dicyclopentadiene—*Journal of Polymer Science A* **40**, 2373–2383 (2002)	Feb. 2002
1001	Dolbow, J. E., E. Fried, and A. Q. Shen	Point defects in nematic gels: The case for hedgehogs—*Archive for Rational Mechanics and Analysis*, in press (2004)	Feb. 2002
1002	Riahi, D. N.	Nonlinear steady convection in rotating mushy layers—*Journal of Fluid Mechanics* **485**, 279–306 (2003)	Mar. 2002
1003	Carlson, D. E., E. Fried, and S. Sellers	The totality of soft-states in a neo-classical nematic elastomer—*Journal of Elasticity* **69**, 169–180 (2003) with revised title	Mar. 2002
1004	Fried, E., and R. E. Todres	Normal-stress differences and the detection of disclinations in nematic elastomers—*Journal of Polymer Science B: Polymer Physics* **40**, 2098–2106 (2002)	June 2002
1005	Fried, E., and B. C. Roy	Gravity-induced segregation of cohesionless granular mixtures—*Lecture Notes in Mechanics*, in press (2002)	July 2002
1006	Tomkins, C. D., and R. J. Adrian	Spanwise structure and scale growth in turbulent boundary layers—*Journal of Fluid Mechanics* (submitted)	Aug. 2002
1007	Riahi, D. N.	On nonlinear convection in mushy layers: Part 2. Mixed oscillatory and stationary modes of convection—*Journal of Fluid Mechanics*, in press (2004)	Sept. 2002
1008	Aref, H., P. K. Newton, M. A. Stremler, T. Tokieda, and D. L. Vainchtein	Vortex crystals—*Advances in Applied Mathematics* **39**, in press (2002)	Oct. 2002
1009	Bagchi, P., and S. Balachandar	Effect of turbulence on the drag and lift of a particle—*Physics of Fluids*, in press (2003)	Oct. 2002
1010	Zhang, S., R. Panat, and K. J. Hsia	Influence of surface morphology on the adhesive strength of aluminum/epoxy interfaces—*Journal of Adhesion Science and Technology* **17**, 1685–1711 (2003)	Oct. 2002
1011	Carlson, D. E., E. Fried, and D. A. Tortorelli	On internal constraints in continuum mechanics—*Journal of Elasticity* **70**, 101–109 (2003)	Oct. 2002
1012	Boyland, P. L., M. A. Stremler, and H. Aref	Topological fluid mechanics of point vortex motions—*Physica D* **175**, 69–95 (2002)	Oct. 2002

List of Recent TAM Reports (cont'd)

No.	*Authors*	*Title*	*Date*
1013	Bhattacharjee, P., and D. N. Riahi	Computational studies of the effect of rotation on convection during protein crystallization—*International Journal of Mathematical Sciences*, in press (2004)	Feb. 2003
1014	Brown, E. N., M. R. Kessler, N. R. Sottos, and S. R. White	*In situ* poly(urea-formaldehyde) microencapsulation of dicyclopentadiene—*Journal of Microencapsulation* (submitted)	Feb. 2003
1015	Brown, E. N., S. R. White, and N. R. Sottos	Microcapsule induced toughening in a self-healing polymer composite—*Journal of Materials Science* (submitted)	Feb. 2003
1016	Kuznetsov, I. R., and D. S. Stewart	Burning rate of energetic materials with thermal expansion—*Combustion and Flame* (submitted)	Mar. 2003
1017	Dolbow, J., E. Fried, and H. Ji	Chemically induced swelling of hydrogels—*Journal of the Mechanics and Physics of Solids*, in press (2003)	Mar. 2003
1018	Costello, G. A.	Mechanics of wire rope—Mordica Lecture, Interwire 2003, Wire Association International, Atlanta, Georgia, May 12, 2003	Mar. 2003
1019	Wang, J., N. R. Sottos, and R. L. Weaver	Thin film adhesion measurement by laser induced stress waves—*Journal of the Mechanics and Physics of Solids* (submitted)	Apr. 2003
1020	Bhattacharjee, P., and D. N. Riahi	Effect of rotation on surface tension driven flow during protein crystallization—*Microgravity Science and Technology* **14**, 36–44 (2003)	Apr. 2003
1021	Fried, E.	The configurational and standard force balances are not always statements of a single law—*Proceedings of the Royal Society* (submitted)	Apr. 2003
1022	Panat, R. P., and K. J. Hsia	Experimental investigation of the bond coat rumpling instability under isothermal and cyclic thermal histories in thermal barrier systems—*Proceedings of the Royal Society of London A* **460**, 1957–1979 (2003)	May 2003
1023	Fried, E., and M. E. Gurtin	A unified treatment of evolving interfaces accounting for small deformations and atomic transport: grain-boundaries, phase transitions, epitaxy—*Advances in Applied Mechanics*, in press (2003)	May 2003
1024	Dong, F., D. N. Riahi, and A. T. Hsui	On similarity waves in compacting media—*Horizons in Physics*, in press (2003)	May 2003
1025	Liu, M., and K. J. Hsia	Locking of electric field induced non-180° domain switching and phase transition in ferroelectric materials upon cyclic electric fatigue—*Applied Physics Letters* **83**, 3978–3980 (2003)	May 2003
1026	Liu, M., K. J. Hsia, and M. Sardela Jr.	In situ X-ray diffraction study of electric field induced domain switching and phase transition in PZT-5H—*Journal of the American Ceramics Society* (submitted)	May 2003
1027	Riahi, D. N.	On flow of binary alloys during crystal growth—*Recent Research Development in Crystal Growth*, in press (2003)	May 2003
1028	Riahi, D. N.	On fluid dynamics during crystallization—*Recent Research Development in Fluid Dynamics*, in press (2003)	July 2003
1029	Fried, E., V. Korchagin, and R. E. Todres	Biaxial disclinated states in nematic elastomers—*Journal of Chemical Physics* **119**, 13170–13179 (2003)	July 2003
1030	Sharp, K. V., and R. J. Adrian	Transition from laminar to turbulent flow in liquid filled microtubes—*Physics of Fluids* (submitted)	July 2003
1031	Yoon, H. S., D. F. Hill, S. Balachandar, R. J. Adrian, and M. Y. Ha	Reynolds number scaling of flow in a Rushton turbine stirred tank: Part I—Mean flow, circular jet and tip vortex scaling—*Chemical Engineering Science* (submitted)	Aug. 2003
1032	Raju, R., S. Balachandar, D. F. Hill, and R. J. Adrian	Reynolds number scaling of flow in a Rushton turbine stirred tank: Part II—Eigen-decomposition of fluctuation—*Chemical Engineering Science* (submitted)	Aug. 2003
1033	Hill, K. M., G. Gioia, and V. V. Tota	Structure and kinematics in dense free-surface granular flow—*Physical Review Letters*, in press (2003)	Aug. 2003

List of Recent TAM Reports (cont'd)

No.	*Authors*	*Title*	*Date*
1034	Fried, E., and S. Sellers	Free-energy density functions for nematic elastomers—*Journal of the Mechanics and Physics of Solids* **52**, 1671–1689 (2004)	Sept. 2003
1035	Kasimov, A. R., and D. S. Stewart	On the dynamics of self-sustained one-dimensional detonations: A numerical study in the shock-attached frame—*Physics of Fluids* (submitted)	Nov. 2003
1036	Fried, E., and B. C. Roy	Disclinations in a homogeneously deformed nematic elastomer—*Nature Materials* (submitted)	Nov. 2003
1037	Fried, E., and M. E. Gurtin	The unifying nature of the configurational force balance—*Mechanics of Material Forces* (P. Steinmann and G. A. Maugin, eds.), in press (2003)	Dec. 2003
1038	Panat, R., K. J. Hsia, and J. W. Oldham	Rumpling instability in thermal barrier systems under isothermal conditions in vacuum—*Philosophical Magazine*, in press (2004)	Dec. 2003
1039	Cermelli, P., E. Fried, and M. E. Gurtin	Sharp-interface nematic–isotropic phase transitions without flow—*Archive for Rational Mechanics and Analysis* (submitted)	Dec. 2003
1040	Yoo, S., and D. S. Stewart	A hybrid level-set method in two and three dimensions for modeling detonation and combustion problems in complex geometries—*Combustion Theory and Modeling* (submitted)	Feb. 2004
1041	Dienberg, C. E., S. E. Ott-Monsivais, J. L. Ranchero, A. A. Rzeszutko, and C. L. Winter	Proceedings of the Fifth Annual Research Conference in Mechanics (April 2003), TAM Department, UIUC (E. N. Brown, ed.)	Feb. 2004
1042	Kasimov, A. R., and D. S. Stewart	Asymptotic theory of ignition and failure of self-sustained detonations—*Journal of Fluid Mechanics* (submitted)	Feb. 2004
1043	Kasimov, A. R., and D. S. Stewart	Theory of direct initiation of gaseous detonations and comparison with experiment—*Proceedings of the Combustion Institute* (submitted)	Mar. 2004
1044	Panat, R., K. J. Hsia, and D. G. Cahill	Evolution of surface waviness in thin films via volume and surface diffusion—*Journal of Applied Physics* (submitted)	Mar. 2004
1045	Riahi, D. N.	Steady and oscillatory flow in a mushy layer—*Current Topics in Crystal Growth Research*, in press (2004)	Mar. 2004
1046	Riahi, D. N.	Modeling flows in protein crystal growth—*Current Topics in Crystal Growth Research*, in press (2004)	Mar. 2004
1047	Bagchi, P., and S. Balachandar	Response of the wake of an isolated particle to isotropic turbulent cross-flow—*Journal of Fluid Mechanics* (submitted)	Mar. 2004
1048	Brown, E. N., S. R. White, and N. R. Sottos	Fatigue crack propagation in microcapsule toughened epoxy—*Journal of Materials Science* (submitted)	Apr. 2004
1049	Zeng, L., S. Balachandar, and P. Fischer	Wall-induced forces on a rigid sphere at finite Reynolds number—*Journal of Fluid Mechanics* (submitted)	May 2004
1050	Dolbow, J., E. Fried, and H. Ji	A numerical strategy for investigating the kinetic response of stimulus-responsive hydrogels—*Journal of the Mechanics and Physics of Solids* (submitted)	June 2004
1051	Riahi, D. N.	Effect of permeability on steady flow in a dendrite layer—*Journal of Porous Media* (submitted)	July 2004
1052	Cermelli, P., E. Fried, and M. E. Gurtin	Transport relations for surface integrals arising in the formulation of balance laws for evolving fluid interfaces—*Journal of Fluid Mechanics* (submitted)	Sept. 2004
1053	Stewart, D. S., and A. R. Kasimov	Theory of detonation with an embedded sonic locus—*SIAM Journal on Applied Mathematics* (submitted)	Oct. 2004
1054	Stewart, D. S., K. C. Tang, S. Yoo, M. Q. Brewster, and I. R. Kuznetsov	Multi-scale modeling of solid rocket motors: Time integration methods from computational aerodynamics applied to stable quasi-steady motor burning—*Proceedings of the 43rd AIAA Aerospace Sciences Meeting and Exhibit* (January 2005), Paper AIAA-2005-0357 (2005)	Oct. 2004